Kinetics and Products of Heterogeneous Reaction of HONO with Fe2O3 and Arizona Test Dust

ARTICLE *in* ENVIRONMENTAL SCIENCE & TECHNOLOGY · MAY 2013

Impact Factor: 5.33 · DOI: 10.1021/es400794c · Source: PubMed

3 AUTHORS:

Atallah El Zein
Université du Littoral Côte d'Opale (ULCO)
13 PUBLICATIONS **119** CITATIONS
SEE PROFILE

Manolis N Romanias
Ecole des Mines de Douai
25 PUBLICATIONS **99** CITATIONS
SEE PROFILE

Yuri Bedjanian
CNRS Orleans Campus
67 PUBLICATIONS **853** CITATIONS
SEE PROFILE

Environmental Science & Technology

Article

pubs.acs.org/est

Kinetics and Products of Heterogeneous Reaction of HONO with Fe_2O_3 and Arizona Test Dust.

Atallah El Zein, Manolis N. Romanias, and Yuri Bedjanian*

Institut de Combustion, Aérothermique, Réactivité et Environnement (ICARE), CNRS, 45071 Orléans Cedex 2, France

Supporting Information

ABSTRACT: Kinetics and products of the reaction of HONO with solid films of Fe_2O_3 and Arizona Test Dust (ATD) were investigated using a low pressure flow reactor (1 − 10 Torr) combined with a modulated molecular beam mass spectrometer. The reactive uptake of HONO was studied as a function of HONO concentration ($[HONO]_0 = (0.6 - 15.0) \times 10^{12}$ molecules cm^{-3}), relative humidity (RH = 3×10^{-4} − 84.1%) and temperature (T = 275 − 320 K). Initial reactive uptake coefficients were found to be similar under dark conditions and in the presence of UV irradiation ($J_{NO2} = 0.012\ s^{-1}$) and independent of the HONO concentration and temperature. In contrast, the relative humidity (RH) was found to have a strong impact on the uptake coefficients: γ (ATD) = 3.8×10^{-6} $(RH)^{-0.61}$ and γ (Fe_2O_3) = 1.7×10^{-6} $(RH)^{-0.62}$ (γ calculated with BET surface area, 30% conservative uncertainty). In both reactions of HONO studied, NO_2 and NO were observed as gaseous products with yields of (60 ± 9) and (40 ± 6) %, respectively, independent of relative humidity, temperature, concentration of HONO and UV irradiation intensity. The observed data point to minor importance of the HONO uptake on mineral aerosol compared with other known sinks of HONO in the atmosphere, which are its dry deposition and photolysis in night-time and during the day, respectively.

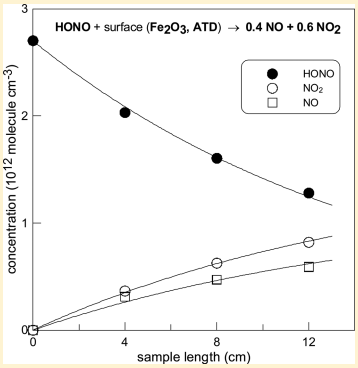

INTRODUCTION

Nitrous acid is an important atmospheric trace species representing a significant day time source (via photolysis) of OH radical, the major atmospheric oxidant. HONO affects the HO_x and NO_x atmospheric budgets, and, consequently, tropospheric ozone formation and oxidative capacity of the troposphere.[1,2] Even so the mechanisms of HONO formation in the atmosphere are still not completely understood. One current issue in the chemistry of HONO is that the models fail to reproduce unexpectedly high daytime concentrations of HONO observed in the field studies, indicating the existence of new, yet unknown, daytime sources of HONO.[3] Heterogeneous processes, including those on humid surfaces, thought to be the major source of HONO in the atmosphere, were intensively studied in the laboratory and several mechanisms of HONO formation on aerosol and ground surface have been proposed.[3]

In competition with heterogeneous formation of HONO, the atmospheric aerosol can also act as a sink for gaseous HONO via heterogeneous transformation of nitrous acid on the aerosol surface. The kinetic and mechanistic data on HONO interaction with different surfaces seem to be very useful, not only for atmospheric implications but also for laboratory studies of the HONO forming heterogeneous processes where secondary surface reactions of HONO may have an impact on the occurring chemistry and final HONO yields. The available information on the nature, rate, and products of HONO interaction with solid surfaces of atmospheric interest is very scarce and seems to be limited to a few studies carried out with ice[4−8] and soot surfaces.[9,10] In addition, there have been several studies of the loss of HONO on "laboratory" surfaces such as Pyrex[11,12] and borosilicate glass.[13]

In recent studies from our group new data on the uptake of HONO to TiO_2[14,15] and Al_2O_3[16] surfaces were reported. In the present paper, the systematic studies of the kinetics and products of the heterogeneous interaction of HONO with different constituents of mineral aerosols are extended to the interaction of HONO with Fe_2O_3 and Arizona Test Dust (ATD) surfaces. Iron oxide is an important component of mineral dust often used as a model compound to mimic the surface reactivity of mineral aerosols and ATD is a mixture of metal oxides, which are generally present in atmospheric mineral aerosols in various proportions. The uptake coefficients of HONO to ATD and Fe_2O_3 surfaces and the yields of the reaction products were measured as a function of HONO concentration, relative humidity (RH) and temperature under dark conditions and in the presence of UV irradiation.

EXPERIMENTAL SECTION

The interaction of HONO with solid ATD and Fe_2O_3 films was studied at 1−10 Torr total pressure (He being used as a carrier gas) using the flow tube technique in combination with a quadrupole mass spectrometer for monitoring of the gas phase.

Received: February 20, 2013
Revised: May 21, 2013
Accepted: May 23, 2013
Published: May 23, 2013

The experimental equipment and approach used for the kinetic measurements were described in previous publications from this group.[10,14,17] The main reactor (Supporting Information (SI), Figure S1) consisted of a Pyrex tube (40 cm length and 2.4 cm i.d.) with a jacket for the thermostatted liquid circulation. Experiments were carried out using a coaxial configuration of the flow reactor, a Pyrex tube with the outer mineral coating being introduced into the main reactor along its axis. The coated tube could be moved which allowed the variation of the solid film length exposed to gas phase reactant and consequently of the reaction time (SI, Figure S1). The temperature of the sample could be changed by two methods: by circulating thermostatted water or ethanol inside the tube coated with the sample or by means of a coaxial cylindrical heater (5 mm o.d., 20 cm length) which could be introduced inside the support tube. The reactor was surrounded by 6 lamps (Sylvania BL350, 8 W, 315 − 400 nm with peak at 352 nm). The actinic flux inside the reactor was not measured in the present study, however, in order to characterize the irradiance intensity in the reactor we have directly measured the NO_2 photolysis frequency, J_{NO2}, as a function of the number of lamps switched on. The values of J_{NO2} were found to be between 0.002 and 0.012 s^{-1} for 1 to 6 lamps switched on, respectively.[17]

Solid films of Fe_2O_3 (Sigma-Aldrich, < 5 μm particle diameter) and ATD (Powder Technology Inc., nominal 0−3 μm ATD) were deposited on the outer surface of a cylindrical Pyrex tube (0.9 cm o.d.) using a suspension of the mineral powders in ethanol. The tube was first immersed into the suspension, then withdrawn and dried with a fan heater. As a result rather homogeneous (to eye) films of the minerals were formed at the Pyrex surface. In order to eliminate the possible residual traces of ethanol, prior to uptake experiments, the freshly prepared coatings were heated at (150−170) °C under pumping in the main reactor for 20−30 min by means of a coaxial cylindrical heater introduced inside the tube coated with the sample. The mass of the solid samples was measured with a high accuracy mass balance upon their mechanical removing from the glass tube at the end of the uptake experiments. BET surface areas of ATD and iron oxide powders were determined using a Quantachrome−Autosorb-1-MP-6 apparatus and nitrogen as adsorbate gas and were found to be 85 ± 10 m^2g^{-1} and 11 ± 2 m^2g^{-1}, respectively.

Gaseous nitrous acid was produced in the heterogeneous reaction of HCl with $NaNO_2$:

$$HCl + NaNO_2 \rightarrow HONO + NaCl$$

HCl diluted in He being passed through a column containing $NaNO_2$ crystals. Heterogeneously formed HONO was introduced into the main reactor through its side arm and was detected at its parent peak as $HONO^+$ (m/z = 47). Under the Experimental conditions used this source of HONO was found to be free of residual concentration of HCl. Monitoring of the HCl concentration by mass spectrometry confirmed that HCl was completely consumed in reaction with $NaNO_2$ and did not reach the main reactor. This HONO source is known to be free of NO_2 and HNO_3.[18] Indeed, in the present work, no signals were detected at m/z = 46 (NO_2^+), 62 (NO_3^+), and 63 (HNO_3^+) when HONO was present in the reactor. However, measurable concentration of NO coming from the HONO source was detected (10−20% of [HONO]), in agreement with previously reported results.[18] The absolute calibration of the mass spectrometer for HONO consisted in chemical conversion of HONO to NO_2 via fast reaction with fluorine atoms with subsequent detection and measurement of NO_2 concentration formed:[18]

$$F + HONO \rightarrow HF + NO_2$$

H_2O was introduced into the reactor from a bubbler containing thermostatted (T = 298 K) deionized water. The concentrations of H_2O in the reactor were determined by calculating the H_2O flow rate from the total (H_2O + He) and H_2O vapor pressures in H_2O bubbler and the measured flow rate of He through the bubbler. The partial pressure of water vapor in the bubbler was measured with VAISALA DRYCAP DMT340 dew-point transmitter. The concentrations of the other stable species, in particular those of the reaction products NO and NO_2, were calculated from their flow rates obtained from the measurements of the pressure drop in calibrated volume flasks with the species diluted in helium. All species were detected at their parent peaks. NO_2 and HONO were found to contribute to the mass peak m/z =30, parent peak of NO, due to their fragmentation in the ion source of the mass spectrometer, which was operated at 25−30 eV. These contributions were determined and subtracted from the total signal at m/z = 30.

RESULTS AND DISCUSSION

Kinetics of HONO Uptake. Figure 1 displays typical uptake profiles of HONO upon introduction of mineral sample into the reaction zone (in contact with HONO, $t \approx 2$ min). Fast initial consumption is followed by a rapid decrease of the HONO loss rate (sharp initial peak in Figure 1, solid line) to quasi steady state, which in turn slowly decreases with time. When the sample is withdrawn from the reaction zone ($t \approx 26$ min), that is, when HONO is no longer in contact with the mineral surface, the HONO concentration rapidly recovers to its initial value. Thus, no additional HONO desorbed from the surface was observed, indicating the reactive nature of the HONO uptake. The reactive uptake of HONO was confirmed by the detection of the reaction products, NO_2 and NO, with the nearly unity total yield for the sum of these gas phase products (see below). It should be noted that no products

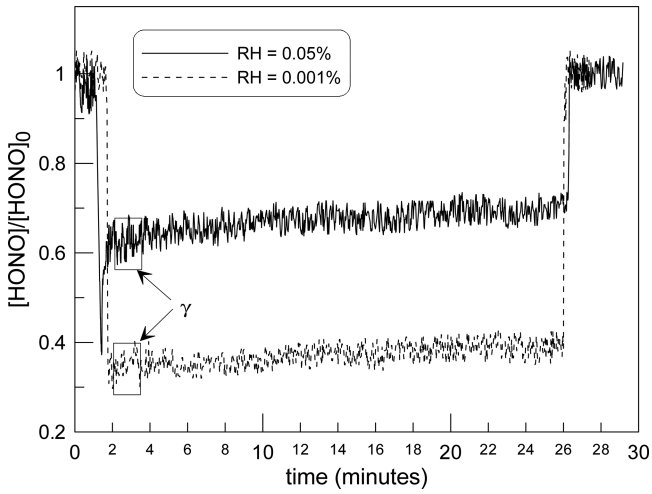

Figure 1. Time-dependent HONO loss in reaction of HONO with ATD surface: T = 300 K, P = 1 Torr, $[HONO]_0 \approx 2\times 10^{12}$ molecules cm^{-3}, flow velocity =1540 cm s^{-1}; solid line: RH = 0.05%, sample mass = 1.8 mg cm^{-1} × 10 cm; dashed line: RH = 0.001%, sample mass = 0.5 mg cm^{-1} × 10 cm.

formation occurred at the first stage of the heterogeneous reaction despite significant initial consumption of HONO. A delayed production of NO_2 and NO was observed, their maximum yield being reached after 1−2 min of mineral sample exposure to HONO and then remained unchanged (at least, up to 3 h, maximum exposure time in our experiments). Thereby, in the determination of the uptake coefficient, the rapid initial non reactive stage of the heterogeneous interaction was not considered and the measurements were focused on the initial value of the reactive uptake coefficient as outlined in Figure 1. The uptake coefficient was determined as the probability of irreversible loss of HONO molecules per collision with the solid surface:

$$\gamma = \frac{4k'}{\omega} \times \frac{V}{S}$$

where k' (in s^{-1}) is the first order rate constant of the HONO heterogeneous loss, ω is the average molecular speed, V is the volume of the reaction zone, and S is the surface area of the mineral coating.

The values of k' were determined from the kinetics of HONO consumption. Example of HONO loss kinetics in heterogeneous reaction with the surface of Fe_2O_3 are shown in Figure 2 and SI Figure S2. Each of the kinetics shown was

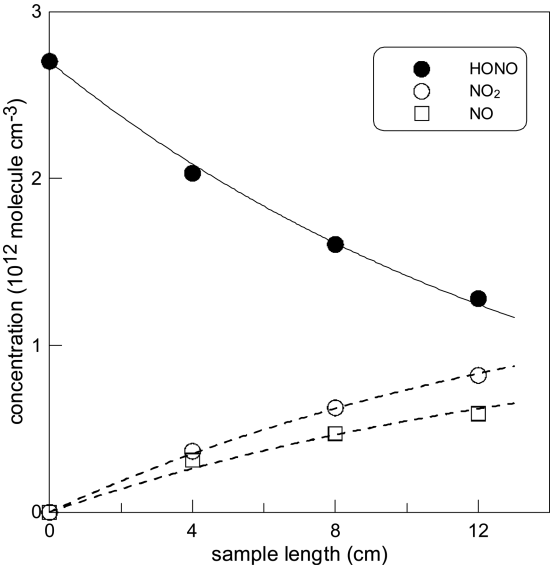

Figure 2. Examples of kinetics of HONO consumption and products (NO and NO_2) formation on Fe_2O_3 surface: T = 300K, P = 1 Torr, flow velocity =1540 cm s^{-1}, RH = 0.001%, sample mass = 7.9 mg cm^{-1}.

obtained with one mineral film in a single experiment by varying the length of the mineral film in contact with HONO, which is equivalent to varying the reaction time. The kinetic runs were measured under quasi steady state uptake conditions, where decrease of the uptake with time is rather slow and could be considered as negligible during a few minutes of the acquisition time. The kinetics of HONO consumption was found to be exponential (solid lines in Figure 2 and SI Figure S2) and the rate constant of the HONO decay on the surface was calculated assuming the first-order kinetics regime, k' being determined as:

$$k' = -\frac{\mathrm{dln}([\mathrm{HONO}])}{\mathrm{d}t}$$

where t is the reaction time defined by the sample length/flow velocity ratio. The values of the first-order rate constants, k', determined from the decays of HONO were corrected for the diffusion limitation in the HONO radial transport from the volume to the reactive surface.[19−21] For the diffusion coefficient of HONO the value of D = 490 Torr cm^2 s^{-1} at T = 300 K measured in our recent study[14] was used, assuming $T^{1.75}$-dependence of D on temperature. The diffusion corrections applied to k' were generally within 10% and reached nearly 30% for a few highest k' measured on ATD surface under dry conditions.

Mass Dependence of k'. In order to determine the surface area of solid samples available for the interaction with HONO, the heterogeneous loss rate of HONO was measured as a function of the thickness of the deposited mineral film. The results are displayed in Figure 3 as dependences of the rate

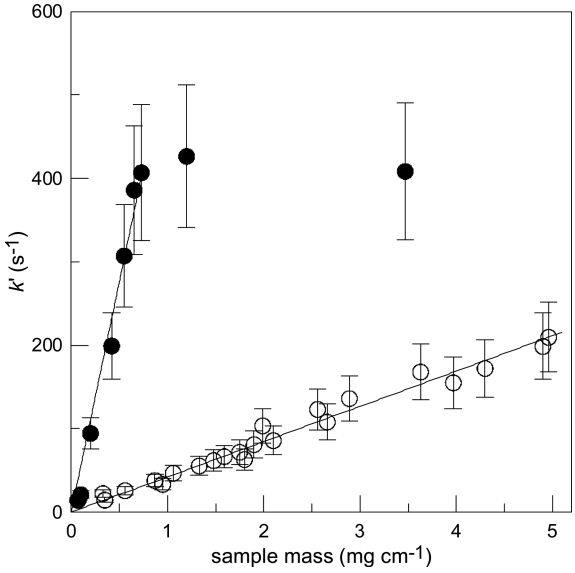

Figure 3. First order rate constant of heterogeneous loss of HONO as a function of the mass of mineral sample (per 1 cm length of the support tube): T = 300 K, $[\mathrm{HONO}]_0 \approx 2\times 10^{12}$ molecules cm^{-3}. Filled and open symbols correspond to the data for ATD (RH ≅ 0.001%) and Fe_2O_3 (RH ≅ 0.0005%), respectively. Error bars represent 20% uncertainty on the measurements of k'.

constant of HONO loss on the mass of ATD and Fe_2O_3 deposited per unity length of the support tube (equivalent to the thickness of the coating). Linear dependence of the reaction rate on the coating thickness is observed for Fe_2O_3 and two regimes are observed for ATD surface: the first one, where k' linearly increases upon increase of the thickness of ATD coating, and the second one (saturation region), where k' is independent of the sample mass. The linear dependence of the reaction rate on mass (thickness) of the reactive film was considered as an indication that the entire surface area of the solid sample is accessible to HONO.[22] Consequently, the uptake measurements in the present study were carried with sample masses corresponding to a "linear regime" of k' (≤0.6 mg cm^{-1} for ATD), and BET surface areas were used for calculations of the uptake coefficients. The linear dependences in Figure 3 provide the following values for the uptake

dx.doi.org/10.1021/es400794c | Environ. Sci. Technol. 2013, 47, 6325−6331

coefficients of HONO under dry conditions (RH ≈ 0.001 and 0.0005% for ATD and Fe_2O_3, respectively) and T = 300 K:

$$\gamma(\mathrm{ATD}) = (2.7 \pm 0.8) \times 10^{-4}$$

$$\gamma(\mathrm{Fe_2O_3}) = (1.6 \pm 0.5) \times 10^{-4}$$

where estimated near 30% uncertainty includes statistical one and those related to the BET surface area and to the measurements of k'. It has to be noted that the values obtained for γ, being calculated with BET surface area, should be considered as lower limits of the uptake coefficients.

Experiments described in this section were carried out with initial concentration of HONO of 2×10^{12} molecules cm^{-3}. Dependence of γ on initial concentration of HONO was verified in separate experiments with $[HONO]_0$ varied in the range 5.8×10^{11} - 1.5×10^{13} molecules cm^{-3}. Under these conditions, the uptake coefficient was found to be independent of $[HONO]_0$. Lack of dependence of the initial uptake coefficient on HONO concentration could be expected. Generally (for first order kinetics) the initial uptake is not expected to be dependent on the gas phase concentration of the reactant since at the initial stage of the surface exposure, the active sites on the surface are not depleted or blocked and are all available for the heterogeneous reaction.

RH Dependence. In this series of experiments the uptake coefficient of HONO was measured as a function of relative humidity. Prior to uptake experiments (contact with HONO), the freshly prepared mineral samples were heated under pumping (as noted in Experimental section) and then exposed during nearly 5 min to water vapor present in the reactor. Longer (up to 30 min) exposure of samples to water vapor had no impact on the observed uptake data, indicating that water to surface adsorption equilibrium was reached during a few minutes. Uptake of HONO on the surface of iron oxide was measured at T = 300 K. Experiments with ATD surface were performed at lower temperature of 275 K in order to provide higher RH, relevant to those in the atmosphere, under relatively low pressures in our flow reactor. The measured uptake coefficients were found to be inversely dependent on the relative humidity (Figure 4). The rather strong negative dependences on RH observed for the uptake coefficients can be well represented by power functions (solid lines in Figure 4):

$$\gamma(\mathrm{ATD}) = 3.8 \times 10^{-6}(\mathrm{RH})^{-0.61}$$

$$\gamma(\mathrm{Fe_2O_3}) = 1.7 \times 10^{-6}(\mathrm{RH})^{-0.62}$$

for RH in the range $(3.9 \times 10^{-4} - 84.1)$ % and $(3.0 \times 10^{-4} - 14.4)$ %, respectively, and with estimated conservative 30% uncertainty on the determination of the uptake coefficient.

Strong inverse dependence on relative humidity observed in the present study for the uptake coefficient of HONO to ATD and Fe_2O_3 is similar to those reported previously for HONO uptake on TiO_2 and Al_2O_3 surfaces under dark conditions (Table 1). Decrease of the HONO loss rate with increasing RH was also observed in previous studies carried out with glass surfaces.[11,13] Moreover, in the work of Kaiser and Wu[11] the rate of HONO loss on the walls of a Pyrex reactor was found to decrease with increasing RH (from 0.2 to 5%) in accordance with an apparent reaction order in water concentration of −0.6, which is identical to the data presented in Table 1. The negative dependence of the HONO uptake rate on water concentration

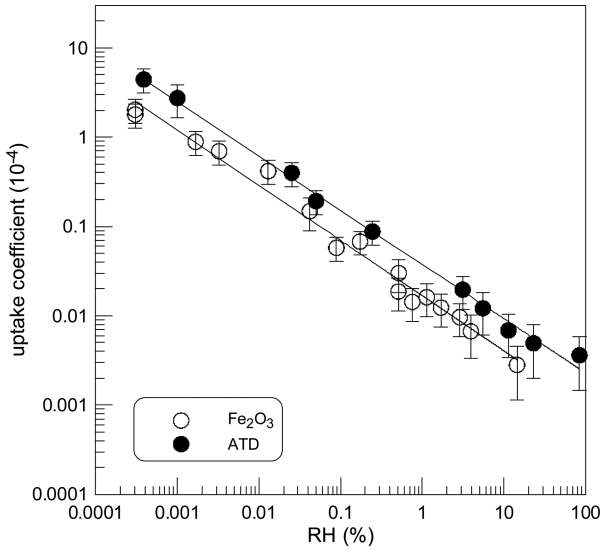

Figure 4. Uptake coefficient as a function of relative humidity: the uptake data for Fe_2O_3 and ATD were measured at T = 300 and 275 K, respectively.

was attributed to competition between HONO and H_2O for the available surface sites.[13]

In previous studies from our group, UV irradiation was found to increase the heterogeneous reactivity of TiO_2[15] and Al_2O_3[16] surfaces. Considering the abundance of these species in Arizona Test Dust (SI, Table S1) and relatively high uptake coefficients of HONO measured on these surfaces in presence of UV light (γ(UV) in Table 1), one could have expected an appreciable effect of the UV irradiation on the uptake of HONO on ATD surface. However, in the present study we have not observed any impact of the UV irradiation (J_{NO2} = 0.002−0.012 s^{-1}) on the uptake of HONO to ATD (and Fe_2O_3) at RH = $(3 \times 10^{-4}$−10) % in the range of the experimental uncertainty on the measurements of γ. Rather strong UV effect observed for titanium oxide[15] could be expected, considering that TiO_2 is known to be an efficient photocatalyst. The observation of the UV effect for the reaction of HONO on Al_2O_3 surfaces[16] was somewhat surprising, since the direct band gap excitation of Al_2O_3 (9 eV or 138 nm) under our experimental conditions was excluded. The observed phenomenon was tentatively attributed to the surface mediated photodegradation of HONO on Al_2O_3 via the mechanism according to which, the chemisorbed species inject electrons to the conduction band of Al_2O_3 upon absorption of UV-A irradiation. This was suggested to be the initial step of the process, the rest of the mechanism being similar to that in semiconductor photocatalysis. The results of the present study indicate that this mechanism is not operative in the interaction of HONO with Fe_2O_3 and SiO_2 (which is about 70% of ATD). Generally, iron oxide has a low photocatalytic activity, even though it has narrow bandgap (2.2 eV), because of its band structure with the conduction band edge lower than the standard redox potential of H_2/H_2O and the valence band edge exceeding the standard redox potential of H_2O/O_2.[23,24] Concerning HONO uptake to ATD surface, the lack of UV effect in this case is really surprising. Although the content of TiO_2 in ATD is 0.5−1%, significant impact of UV irradiation on HONO uptake to ATD surface could be expected, especially in presence of water, considering that the uptake coefficient of HONO on pure TiO_2 surface is photoenhanced by nearly 2 orders of magnitude at RH = 10%

dx.doi.org/10.1021/es400794c | Environ. Sci. Technol. 2013, 47, 6325−6331

Table 1. Summary of Experimental Data for the Uptake Coefficient of HONO on Mineral Oxide Surfaces

material	T (K)	RH (%)	γ(dark) × 10^6	γ(UV) × 10^6	reference
TiO_2	300	0.0003−13.0	$18 \times (RH)^{-0.63}$		El Zein et al.[14]
	280	0.001−60.0		$690 \times (RH)^{-0.3}$	El Zein et al.[15]
Al_2O_3	300	0.0002−10.5	$4.8 \times (RH)^{-0.61}$		Romanias et al.[16]
	280	0.0003−35.4		$17 \times (RH)^{-0.44}$	Romanias et al.[16]
Fe_2O_3	300	0.0003 − 14.4	$1.7 \times (RH)^{-0.62}$	no UV effect	this study
ATD	275	0.0004 − 84.1	$3.8 \times (RH)^{-0.61}$	no UV effect	this study

(Table 1). The non observation of the UV effect on the reactivity of HONO toward ATD surface indicates that care must be taken when applying the uptake data obtained with pure mineral samples to their mixtures. Let us note that similar nonlinear (or "non additivity") effect was observed in previous uptake studies on mineral substrates. Thus Monge et al.[25] measuring the uptake coefficient of NO_2 on TiO_2/SiO_2 mixtures under irradiation have observed S-shaped dependence of the uptake coefficient on content of TiO_2. Another example is the study of Ndour et al.[26] on photoreactivity of NO_2 on mineral dusts originating from different locations of the Sahara desert. The authors have not observed any correlation between TiO_2 content in the mineral dusts (between 0.16 and 0.99 wt %) and extent of the photo enhancement of the NO_2 uptake. Finally, it should be noted that the experiments in present study were performed in the absence of molecular oxygen which is an important species in photocatalysis, forming highly reactive superoxide radical O_2^-. In this respect, additional experiments in oxygen containing environment would be interesting.

Temperature Dependence. Temperature dependence of the uptake coefficient of HONO on the surface of iron oxide measured in the temperature range T = (280−320) K for two relative humidities (RH = 0.1 and 4.0%) is shown in Figure S3 (SI). The choice of the relatively low RH in these experiments was due to inability to reach higher relative humidities at high temperatures in the low pressure flow reactor used. As one can see from the data in SI Figure S3, the uptake coefficient was found to be temperature independent in the range of experimental uncertainty and within the temperature range used. Similar results were observed for HONO uptake on ATD surface, where independent of temperature (T = 275−320 K) uptake coefficient was measured at RH = 5% (SI, Figure S4). For comparison, independent of temperature uptake coefficient of HONO on Al_2O_3[16] and negative temperature dependence of γ on TiO_2 surface (with activation factor = −1400 K)[14,15] were reported previously.

Products Study. NO and NO_2 were observed to be released into the gas phase upon interaction of HONO with Fe_2O_3 and ATD surfaces. Example of the kinetics of the products formation along with the kinetics of HONO decay is shown in Figure 2. The dashed lines fitting experimental data correspond to the following equation:

$$[\text{product}] = \alpha \times [\text{HONO}]_0 \times (1 - \exp(-k't))$$

where k' is the first order rate constant determined from the kinetics of HONO consumption and α is the branching ratio for the product forming reaction channel. The values of α obtained from the best fit to experimental data in Figure 2 were 0.57 and 0.43 for NO_2 and NO, respectively, which corresponds to 100% nitrogen mass balance. Experiments described in this section were focused on the determination of the yields of the reaction products under varied experimental conditions. Typical experiments consisted in the introduction of mineral sample into the reaction zone in contact with HONO and the monitoring of the HONO concentration and those of the two gas phase products formed (NO and NO_2). The yield of the detected products was determined as a ratio of the product concentration formed to the concentration of HONO consumed: product yield = Δ[product]/Δ[HONO].

Figure 5 displays the results of the measurements of the concentrations of NO and NO_2 formed in the reaction of

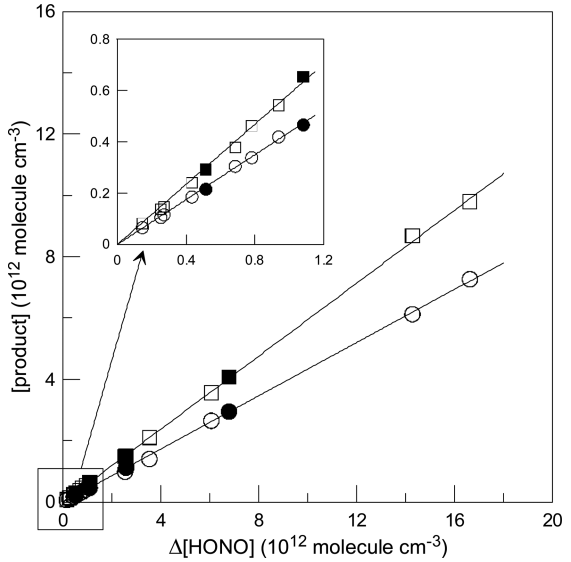

Figure 5. Concentration of the gas phase products, NO (circles) and NO_2 (squares), as a function of the concentration of HONO consumed in reaction with Fe_2O_3: T = 300 K, dry conditions (RH ∼ 0.001%), initial concentration of HONO varied in the range (0.6 − 27.0) × 10^{12} molecules cm^{-3}. Open and filled symbols correspond to the data measured under dark conditions and in the presence of UV irradiation ($J_{NO2} \cong 0.012$ s^{-1}), respectively.

HONO with Fe_2O_3 surface as a function of the consumed concentration of HONO. These data were obtained from different experiments with different concentrations of HONO and at different times of exposure. Initial concentration of HONO was varied in the range $6.0 \times 10^{11} - 2.7 \times 10^{13}$ molecules cm^{-3}. One can note that the impact of the initial concentration of HONO on the yield of the two detected products was negligible. The straight lines in Figure 5 correspond to the linear through origin least-squares fits to the experimental data and provide the branching ratios of 59.5 and 43.4% for the NO_2 and NO forming pathways, respectively. Similarity of the results obtained under dark conditions (open symbols) and under UV irradiation (J_{NO2} = 0.012 s^{-1}, filled

dx.doi.org/10.1021/es400794c | Environ. Sci. Technol. 2013, 47, 6325−6331

symbols) points to a negligible impact of the UV irradiation on the distribution of the products of the heterogeneous reaction.

A series of experiments has been carried out where the influence of humidity and temperature on the yield of the products of the reactions of HONO with Fe_2O_3 and ATD were explored. The impact of temperature (T = 275 − 320 K) on the distribution of the reaction products was found to be negligible on both Fe_2O_3 and ATD surfaces. The corresponding experimental data for HONO − Fe_2O_3 system are detailed in Table S2 (SI). The RH dependence of the yields of the reaction products is shown in Figure 6. One can note that the variation

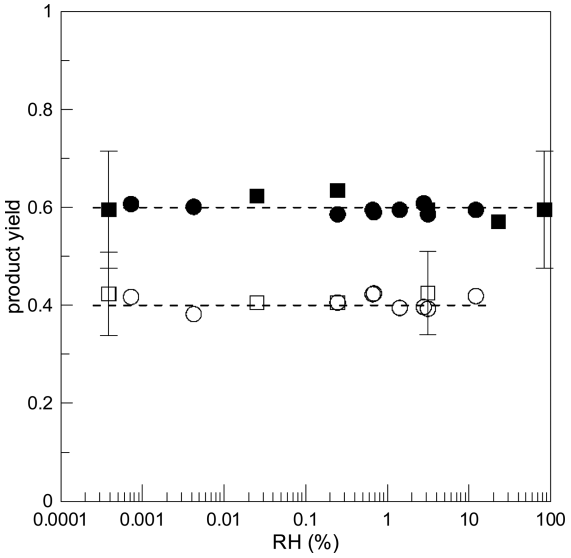

Figure 6. Branching ratio of the NO (open symbols) and NO_2 (filled symbols) forming pathways of the reaction of HONO with Fe_2O_3 (circles) and ATD (squares) surfaces as a function of relative humidity.

of the concentration of water vapor by more than 5 orders of magnitude was found to have no impact on the yields of the products of the heterogeneous reactions. The dashed lines in Figure 6 correspond to mean values of the measured NO_2 and NO yields: 0.60 and 0.41, respectively.

NO_2 and NO being the products of the title reactions, the question arises whether the secondary reactions of these species could affect the results of the HONO uptake and reaction products measurements. Reaction of NO_2 with mineral oxides was quite intensively studied. The values of the initial uptake coefficient reported in the literature for different surfaces under dry conditions are in the range 10^{-5}−10^{-7},[27] that is much lower compared with uptake coefficient of HONO measured in the present study. However, with respect to the present work, the information needed is that on the reactivity of NO_2 in presence of HONO in the reactive system. To check this point we have carried out two types of reference experiments, which consisted of monitoring of NO_2 uptake in presence of HONO on freshly prepared surface and in the absence of HONO, however on pretreated with HONO surface. It was observed that upon introduction of the fresh mineral sample in contact with NO_2/HONO (≈ 1: 4), NO_2 concentration first decreased, than rapidly (∼min) recovered to the level exceeding its initial concentration (due to NO_2 production in heterogeneous reaction of HONO). Presence of NO_2 in the reactive system had no impact on the uptake of HONO. The yield of NO_2 calculated as $([NO_2]\text{-}[NO_2]_0)/\Delta[HONO]$ was found to be independent of the exposure time and similar to that observed in experiments without NO_2 addition. These data suggest an insignificant effect of the NO_2 uptake, at least, for exposure times relevant to experiments on HONO uptake. Further evidence of this was the lack of observable uptake of NO_2 (and NO) on both Fe_2O_3 and ATD surfaces pretreated with HONO.

In summary, two gas phase products, NO_2 and NO, were found to be formed in the heterogeneous reactions of HONO with respective yields of (60 ± 9) and (40 ± 6) %, similar for both ATD and Fe_2O_3 surfaces. The branching ratios for the NO and NO_2 forming reaction pathways were shown to be independent of temperature (T = 275−320 K), relative humidity (0.0004−84.1%) and UV irradiation. Similar results were observed in previous studies of the interaction of HONO with Al_2O_3 and TiO_2.[14,16] For the reaction of HONO with unconditioned glass cell, Syomin and Finlayson-Pitts[13] reported equal yields for NO and NO_2 under dry conditions. In addition, these authors observed that with increasing RH the formation of NO was favored, and NO yield was greater than 90% at 50% RH. They reported that the mechanistic basis for the change in product yields as RH increases is not clear. In the present study the yields of the products of HONO reaction with ATD and Fe_2O_3 surface were found to be independent of the relative humidity up to RH = 84%. This observation as well as non equal yields of NO and NO_2 observed in the present study seem to indicate that the reactive mechanisms involved in the interaction of HONO with glass and mineral oxides are (at least partly) different. The interaction of HONO with the surfaces of mineral oxides can proceed via oxidation/reduction reactions:[16]

$$HONO + SS \rightarrow NO_2 + H^+ + \text{reduced SS}$$

$$HONO + H^+ + \text{reduced SS} \rightarrow NO + H_2O + SS$$

where SS denotes surface site.

Atmospheric Implications. The results obtained for the uptake of HONO on Arizona Test Dust (mimicking chemical composition of the atmospheric mineral aerosol) can be used for comparison of the rate of heterogeneous loss of HONO under atmospheric conditions with other removal processes of HONO in the atmosphere. Using the value of $\gamma(ATD) \approx 5 \times 10^{-7}$ measured at 30% RH and aerosol surface loading, S/V, of $10^{-6} - 10^{-5}$ cm^{-1},[28,29] typical for rural and urban atmosphere and in accordance with

$$k' = \frac{\omega\gamma}{4}\frac{S}{V}$$

the calculated value of HONO loss rate on mineral aerosol is k' ∼ $(4 \times 10^{-9} - 4 \times 10^{-8})$ s^{-1}. This result enables the comparison with other known sinks of HONO in the atmosphere, which are its dry deposition and photolysis in night-time and during the day, respectively. The values reported for the deposition velocity of HONO range from 0.077 to 3 cm s^{-1} (Li et al.[30] and refs therein) which leads to the HONO deposition rate between 7.7×10^{-6} and 3×10^{-4} s^{-1} for 100 m height of the well mixed layer. As one can see, the rate of HONO loss on aerosols estimated above is much lower than the dry deposition rate of HONO and is also negligible compared to the photolysis rate of HONO of $\sim 1.3 \times 10^{-3}$ s^{-1}.[31] Thus the contribution of mineral aerosol to the total HONO loss in the atmosphere either during the day or night-time can be considered as negligible. In conclusion, it can be noted that although HONO reaction with mineral oxides has a limited atmospheric impact, the kinetic and, especially, product

dx.doi.org/10.1021/es400794c | Environ. Sci. Technol. 2013, 47, 6325−6331

data from the present study seems to be very useful and should be accounted for in laboratory studies of potential heterogeneous sources of nitrous acid.

■ ASSOCIATED CONTENT

Supporting Information

Four Figures (diagram of the photoreactor, examples of kinetics of HONO loss, dependences of HONO uptake to Fe_2O_3 and ATD on temperature) and two Tables (chemical composition of ATD and product yield in reaction of HONO with Fe_2O_3 as a function of temperature). This information is available free of charge via the Internet at http://pubs.acs.org.

■ AUTHOR INFORMATION

Corresponding Author

*Phone: +33-238-255-474; rfax: +33-238-696-004; e-mail: yuri.bedjanian@cnrs-orleans.fr.

Notes

The authors declare no competing financial interest.

■ ACKNOWLEDGMENTS

This study was supported by LEFE−CHAT programme of CNRS (Photona project) and ANR from Photodust grant. A.E..Z. is very grateful to région Centre for financing his PhD grant.

■ REFERENCES

(1) Calvert, J.; Yarwood, G.; Dunker, A. An evaluation of the mechanism of nitrous acid formation in the urban atmosphere. *Res. Chem. Intermed.* **1994**, *20* (3), 463−502.

(2) Lammel, G.; Cape, J. N. Nitrous acid and nitrite in the atmosphere. *Chem. Soc. Rev.* **1996**, *25* (5), 361−369.

(3) Kleffmann, J. Daytime sources of nitrous acid (HONO) in the atmospheric boundary layer. *ChemPhysChem* **2007**, *8* (8), 1137−1144.

(4) Fenter, F. F.; Rossi, M. J. Heterogeneous kinetics of HONO on H_2SO_4 solutions and on ice: Activation of HCl. *J. Phys. Chem.* **1996**, *100* (32), 13765−13775.

(5) Chu, L.; Diao, G.; Chu, L. T. Heterogeneous interaction and reaction of HONO on ice films between 173 and 230 K. *J. Phys. Chem. A* **2000**, *104* (14), 3150−3158.

(6) Diao, G.; Chu, L. T. Heterogeneous reactions of HX + HONO and I_2 on ice surfaces: Kinetics and linear correlations. *J. Phys. Chem. A* **2005**, *109* (7), 1364−1373.

(7) Kerbrat, M.; Huthwelker, T.; Bartels-Rausch, T.; Gaggeler, H. W.; Ammann, M. Co-adsorption of acetic acid and nitrous acid on ice. *Phys. Chem. Chem. Phys.* **2010**, *12* (26), 7194−7202.

(8) Kerbrat, M.; Huthwelker, T.; Gäggeler, H. W.; Ammann, M. Interaction of nitrous acid with polycrystalline ice: Adsorption on the surface and diffusion into the bulk. *J. Phys. Chem. C* **2010**, *114* (5), 2208−2219.

(9) Stadler, D.; Rossi, M. J. The reactivity of NO_2 and HONO on flame soot at ambient temperature: The influence of combustion conditions. *Phys. Chem. Chem. Phys.* **2000**, *2* (23), 5420−5429.

(10) Lelièvre, S.; Bedjanian, Y.; Laverdet, G.; Le Bras, G. Heterogeneous reaction of NO_2 with hydrocarbon flame soot. *J. Phys. Chem. A* **2004**, *108* (49), 10807−10817.

(11) Kaiser, E. W.; Wu, C. H. A kinetic study of the gas phase formation and decomposition reactions of nitrous acid. *J. Phys. Chem.* **1977**, *81* (18), 1701−1706.

(12) Ten Brink, H. M.; Spoelstra, H. The dark decay of hono in environmental (SMOG) chambers. *Atmos. Environ.* **1998**, *32* (2), 247−251.

(13) Syomin, D. A.; Finlayson-Pitts, B. J. HONO decomposition on borosilicate glass surfaces: Implications for environmental chamber studies and field experiments. *Phys. Chem. Chem. Phys.* **2003**, *5* (23), 5236−5242.

(14) El Zein, A.; Bedjanian, Y. Reactive uptake of HONO to TiO_2 surface: "dark" reaction. *J. Phys. Chem. A* **2012**, *116* (14), 3665−3672.

(15) El Zein, A.; Bedjanian, Y.; Romanias, M. N. Kinetics and products of HONO interaction with TiO_2 surface under UV irradiation. *Atmos. Environ.* **2013**, *67*, 203−210.

(16) Romanias, M. N.; El Zein, A.; Bedjanian, Y. Reactive uptake of HONO on aluminium oxide surface. *J. Photochem. Photobio. A* **2012**, *250*, 50−57.

(17) El Zein, A.; Bedjanian, Y. Interaction of NO_2 with TiO_2 surface under UV irradiation: Measurements of the uptake coefficient. *Atmos. Chem. Phys.* **2012**, *12* (2), 1013−1020.

(18) Bedjanian, Y.; Lelièvre, S.; Bras, G. L. Kinetic and mechanistic study of the F atom reaction with nitrous acid. *J. Photochem. Photobio. A* **2004**, *168* (1−2), 103−108.

(19) Gershenzon, Y. M.; Grigorieva, V. M.; Zasypkin, A. Y.; Remorov, R. G. In Theory of radial diffusion and first order wall reaction in movable and immovable media, *Proceedings of the 13th International Symposium on Gas Kinetics*, Dublin, Ireland, September 11−16, 1994; University of Dublin: Dublin, Ireland, 1994; pp 420−422.

(20) Gershenzon, Y. M.; Grigorieva, V. M.; Ivanov, A. V.; Remorov, R. G. O_3 and OH sensitivity to heterogeneous sinks of HO_x and CH_3O_2 on aerosol particles. *Faraday Discuss.* **1995**, *100* (100), 83−100.

(21) Bedjanian, Y.; Lelièvre, S.; Le Bras, G. Experimental study of the interaction of HO_2 radicals with soot surface. *Phys. Chem. Chem. Phys.* **2005**, *7* (2), 334−341.

(22) Underwood, G. M.; Li, P.; Usher, C. R.; Grassian, V. H. Determining accurate kinetic parameters of potentially important heterogeneous atmospheric reactions on solid particle surfaces with a knudsen cell reactor. *J. Phys. Chem. A* **2000**, *104* (4), 819−829.

(23) Hoffmann, M. R.; Martin, S. T.; Choi, W.; Bahnemann, D. W. Environmental applications of semiconductor photocatalysis. *Chem. Rev.* **1995**, *95* (1), 69−96.

(24) Xiang, Q.; Yu, J.; Wong, P. K. Quantitative characterization of hydroxyl radicals produced by various photocatalysts. *J. Colloid Interface Sci.* **2011**, *357* (1), 163−167.

(25) Monge, M. E.; D'Anna, B.; George, C. Nitrogen dioxide removal and nitrous acid formation on titanium oxide surfaces-an air quality remediation process? *Phys. Chem. Chem. Phys.* **2010**, *12* (31), 8991−8998.

(26) Ndour, M.; Nicolas, M.; D'Anna, B.; Ka, O.; George, C. Photoreactivity of NO2 on mineral dusts originating from different locations of the Sahara desert. *Phys. Chem. Chem. Phys.* **2009**, *11* (9), 1312−1319.

(27) Crowley, J. N.; Ammann, M.; Cox, R. A.; Hynes, R. G.; Jenkin, M. E.; Mellouki, A.; Rossi, M. J.; Troe, J.; Wallington, T. J. Evaluated kinetic and photochemical data for atmospheric chemistry: Volume V—Heterogeneous reactions on solid substrates. *Atmos. Chem. Phys.* **2010**, *10* (18), 9059−9223.

(28) Wehner, B.; Wiedensohler, A. Long term measurements of submicrometer urban aerosols: Statistical analysis for correlations with meteorological conditions and trace gases. *Atmos. Chem. Phys.* **2003**, *3* (3), 867−879.

(29) Seinfeld, J. H.; Pandis, S. N., *Atmospheric Chemistry and Physics: From Air Pollution to Climate Change*; J. Wiley: New York, 2006.

(30) Li, X.; Brauers, T.; Häseler, R.; Bohn, B.; Fuchs, H.; Hofzumahaus, A.; Holland, F.; Lou, S.; Lu, K. D.; Rohrer, F.; Hu, M.; Zeng, L. M.; Zhang, Y. H.; Garland, R. M.; Su, H.; Nowak, A.; Wiedensohler, A.; Takegawa, N.; Shao, M.; Wahner, A. Exploring the atmospheric chemistry of nitrous acid (HONO) at a rural site in Southern China. *Atmos. Chem. Phys.* **2012**, *12* (3), 1497−1513.

(31) Kraus, A.; Hofzumahaus, A. Field measurements of atmospheric photolysis frequencies for O_3, NO_2, HCHO, CH_3CHO, H_2O_2, and HONO by UV spectroradiometry. *J. Atmos. Chem.* **1998**, *31* (1), 161−180.